

## Photosynthesis

## Biocatalytic Photosynthesis with Water as an Electron Donor

Jungki Ryu,<sup>[a, b]</sup> Dong Heon Nam,<sup>[a]</sup> Sahng Ha Lee,<sup>[a]</sup> and Chan Beum Park\*<sup>[a]</sup>

**Abstract:** Efficient harvesting of unlimited solar energy and its conversion into valuable chemicals is one of the ultimate goals of scientists. With the ever-increasing concerns about sustainable growth and environmental issues, numerous efforts have been made to develop artificial photosynthetic process for the production of fuels and fine chemicals, thus mimicking natural photosynthesis. Despite the research progress made over the decades, the technology is still in its infancy because of the difficulties in kinetic coupling of whole photocatalytic cycles. Herein, we report a new type of artificial photosynthesis system that can avoid such problems by integrally coupling biocatalytic redox reactions with photocatalytic water splitting. We found that photocatalytic water splitting can be efficiently coupled with biocatalytic redox reactions by using tetracobalt polyoxometalate and Rh-based organometallic compound as hole and electron scavengers, respectively, for photoexcited  $[\text{Ru}(\text{bpy})_3]^{2+}$ . Based on these results, we could successfully photosynthesize a model chiral compound (L-glutamate) using a model redox enzyme (glutamate dehydrogenase) upon in situ photoregeneration of cofactors.

Photosynthesis is a series of photophysical and photochemical processes crafted by nature to produce essential biological fuels by converting solar energy into the form of chemical bonds.<sup>[1]</sup> It has many fascinating features such as efficient harvesting of unlimited solar energy and its use, capabilities to perform complex catalytic reactions, and environmental compatibility.<sup>[1,2]</sup> These features are achieved by delicate photosynthetic machinery, where various active components (e.g., light-harvesting dyes, charge-separation components, and redox catalysts) are assembled at nanoscale precision within membrane-bound protein complexes, enabling efficient separation of charges and transfer of redox power.<sup>[1a]</sup> Based on the under-

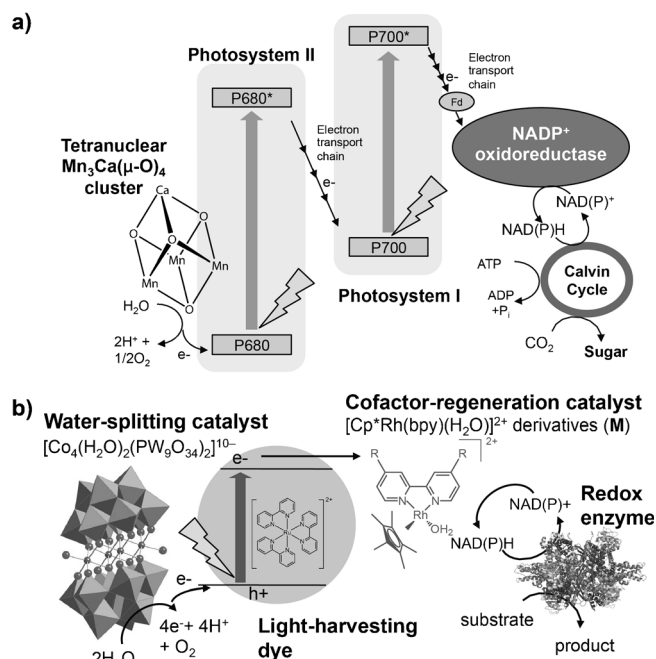


**Figure 1.** Illustrative comparison between a) natural photosynthesis and b) enzyme-coupled artificial photosynthesis for green synthesis of valuable chemicals. In the light reaction, dye molecules (chlorophylls and carotenoids in natural photosynthesis versus  $[\text{Ru}(\text{bpy})_3]^{2+}$  in the present study) are electronically excited upon visible-light irradiation and transfer electrons to the reaction center (NAD<sup>+</sup> oxidoreductases versus **M**) to regenerate nicotinamide cofactor NAD(P)H by reducing its oxidized counterpart NAD(P)<sup>+</sup>. The photocatalytic system oxidized by donating electrons to the reaction center is reduced (and recycled) with electrons supplied from the oxidation of water with a tetranuclear water splitting catalyst ( $\text{Mn}_3\text{CaO}_4$  cluster versus  $[\text{Co}_4(\text{H}_2\text{O})_2(\text{PW}_9\text{O}_{34})_2]^{10-}$ ). The regenerated cofactors are then consumed in the synthesis of complex organic compounds (sugar versus chiral compounds) by redox enzymes in the dark reaction.

standing of the natural photosynthesis mechanism (also known as the Z scheme, Figure 1 a), researchers found that, in principle, chemical fuels such as hydrogen and hydrocarbons can be produced by photocatalytic splitting of water and the reduction of carbon dioxide, respectively, the so-called artificial photosynthesis.<sup>[3]</sup> With the recent energy crisis as well as ever-increasing environmental concerns, numerous efforts have been made to develop a highly efficient artificial photosynthesis system. For example, it has been reported that efficient hydrogen-evolution<sup>[4]</sup> and water-splitting<sup>[5]</sup> catalysts can be developed by mimicking the metal–sulfur cluster of hydrogenase enzymes<sup>[6]</sup> and the tetranuclear  $\text{Mn}_3\text{Ca}(\mu\text{-O})_4$  cluster of the oxygen-evolving complex<sup>[2b,7]</sup> in photosystem II, respectively. Recently, Nam and co-workers reported that the light-harvesting efficiency of dyes can be significantly enhanced by assem-

[a] Dr. J. Ryu, D. H. Nam, Dr. S. H. Lee, Prof. Dr. C. B. Park  
Department of Materials Science and Engineering  
Korea Advanced Institute of Science and Technology (KAIST)  
335 Science Road, Daejeon 305-701 (Republic of Korea)  
E-mail: parkcb@kaist.ac.kr

[b] Dr. J. Ryu  
Current address:  
School of Energy and Chemical Engineering  
Ulsan National Institute of Science and Technology (UNIST)  
50 UNIST-gil, Ulsan 689-798 (Republic of Korea)

Supporting information for this article is available on the WWW under <http://dx.doi.org/10.1002/chem.201403301>.

bling them in a desired arrangement facilitating electronic coupling and charge transport between them.<sup>[8]</sup>

Despite the significant progress made over the past decades, current studies on artificial photosynthesis are still at a very early stage and require a number of scientific breakthroughs for practical applications. For example, only a few studies have reported the development of an integrated photosynthetic system,<sup>[9]</sup> while most current studies have been limited to testing the performance of each component in the form of incomplete half reactions owing to the difficulties in kinetic coupling between catalytic cycles.<sup>[10]</sup> In addition to scientific issues, there still remain a number of technological (e.g., CO<sub>2</sub> capture, separation and storage of gas-phase solar fuels, and development of cheap, efficient, and reliable fuel cells) and economic issues (e.g., efficiency and relative production cost compared to conventional technology) to be addressed for practical application of artificial photosynthesis.<sup>[3b]</sup>

Herein, we report the development of a homogeneous photosynthesis system that can produce fine chemicals through an integral coupling of biocatalytic reactions with photocatalytic water splitting. The new type of artificial photosynthetic process is conceptually very similar to natural photosynthesis, as illustrated in Figure 1. Both processes are composed of independent photocatalytic and biocatalytic reactions connected by redox cycles of nicotinamide cofactors, NAD(P)H. The artificial photosynthetic system is designed to regenerate NAD(P)H from its oxidized counterpart, NAD(P)<sup>+</sup>, through complete photocatalytic redox reaction (i.e., not in the form of half reactions) for the synthesis of complex chemicals, such as chiral alcohols and natural/unnatural amino acids, by using redox enzymes at the expense of in situ regenerated cofactors as a redox equivalent. By utilizing electrostatic interactions between light-harvesting dyes and redox catalysts, we could facilitate efficient separation of charges and directional flow of electrons throughout the overall catalytic cycles, enabling simultaneous photocatalytic oxidation of water and reduction of cofactors.

The photosystem for the regeneration of nicotinamide cofactors consisted of light-harvesting dye [Ru(bpy)<sub>3</sub>]<sup>2+</sup>, a cofactor

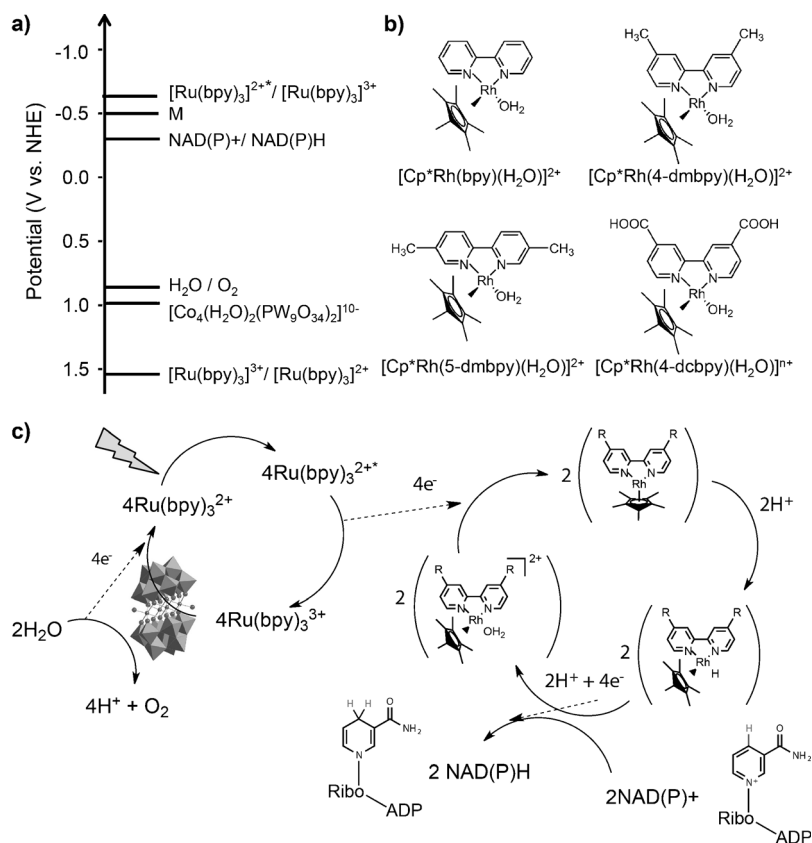


**Figure 2.** a) Diagram showing redox potentials for all the half reactions in the present study. Photoexcited [Ru(bpy)<sub>3</sub>]<sup>2+</sup> has a wide redox potential window, which is large enough to oxidize water and reduce M for the regeneration of NADH cofactors. Note that redox potential of M was determined by cyclic voltammetry (see the Supporting Information, Figure S2 and Table S1). b) Various cofactor regeneration catalysts M having different functional groups on the bipyridine ligand. Note that M can regenerate enzymatically active 1,4-NAD(P)H and prevent the formation of inactive isomers and dimers of NAD(P)H.<sup>[12a]</sup> c) Diagram showing the whole cycle for the photocatalytic regeneration of NAD(P)H cofactors. Note that a key factor for the successful synthesis of target chemicals through complete artificial photosynthesis—not in the form of half reactions—is how to connect the whole catalytic cycles efficiently by facilitating the directional flow of electrons from photocatalytic oxidation of water by Co<sub>4</sub>POM, and then the reduction of cofactors by M, to redox biocatalysis.

regeneration catalyst, and a water-splitting catalyst. We selected [Ru(bpy)<sub>3</sub>]<sup>2+</sup> as a light-harvesting photosensitizer because of its near unity quantum yield, relatively long excited lifetime ( $\tau \sim 1 \mu\text{s}$ ), chemical stability, and its excellent redox properties (Figure 2a).<sup>[11]</sup> A Rh-based electron mediator (M)<sup>[12]</sup> and tetracobalt polyoxometalate [Co<sub>4</sub>(H<sub>2</sub>O)<sub>2</sub>(PW<sub>9</sub>O<sub>34</sub>)<sub>2</sub>]<sup>10-</sup> (Co<sub>4</sub>POM)<sup>[5b,c]</sup> were used as a cofactor regeneration catalyst (Figure 2b and Figures S1 and S2 in the Supporting Information) and a biomimetic tetranuclear water-splitting catalyst (see the Supporting Information, Figure S3–S6), respectively. Before assembling the integrated photosynthetic system, we studied the efficiencies of charge transfer from photoexcited [Ru(bpy)<sub>3</sub>]<sup>2+</sup> dyes to the water-splitting catalyst Co<sub>4</sub>POM and to the conventional cofactor regeneration catalyst, [Cp\*Rh(bpy)(H<sub>2</sub>O)]<sup>2+</sup> (M<sub>bpy</sub>), by analyzing photophysical and chemical properties of [Ru(bpy)<sub>3</sub>]<sup>2+</sup> under various conditions. [Ru(bpy)<sub>3</sub>]<sup>2+</sup> has strong absorbance and photoluminescence (PL) in the visible light region (at around 450 and 600 nm, respectively). By measuring static and dynamic PL spectra (Figure 3a–b and Figure S7 in the Supporting Information), we could calculate the PL lifetime

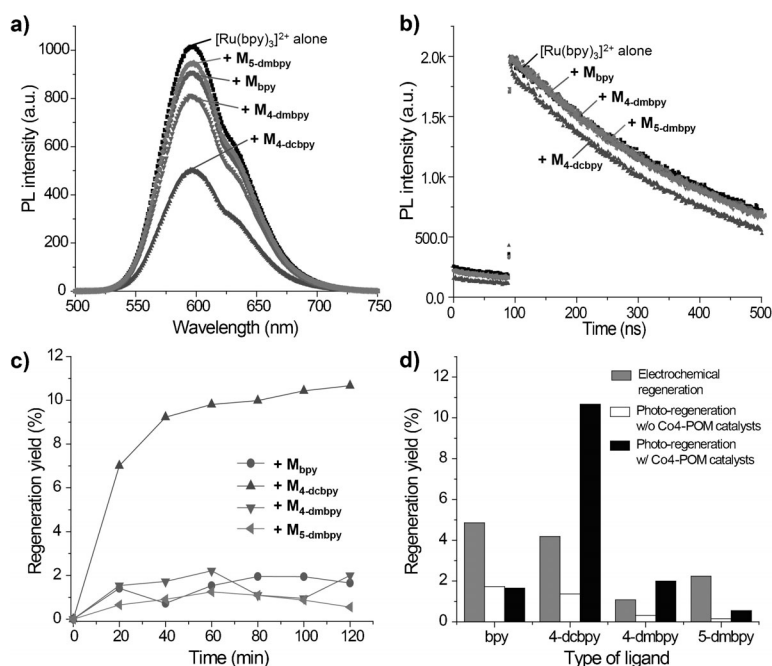


**Figure 3.** a) Static and b) dynamic photoluminescence spectra of  $[\text{Ru}(\text{bpy})_3]^{2+}$  dyes in the presence of **M** having different functional groups. c) Photoregeneration of NADH cofactors achieved by water-splitting reaction with different **M**. d) Comparison between efficiencies of electrochemical and photochemical regeneration of NADH by using different **M**.

| Quencher                                   | PL lifetime <sup>[d]</sup><br>$\tau$ [ns] | Quenching rate coefficient $k_q$ [ $\text{M}^{-1} \text{s}^{-1}$ ] <sup>[e]</sup><br>$I_0/I$ | $\tau_0/\tau$      |
|--|---|--|--------------------|
| control <sup>[a]</sup>                     | 370.97                                    | N.A.   | N.A.               |
| $\text{Co}_4\text{POM}$ <sup>[b]</sup>     | 330.14                                    | $6.97 \times 10^9$   | $1.33 \times 10^9$ |
| $\text{M}_{\text{bpy}}$ <sup>[c]</sup>     | 352.65                                    | $3.23 \times 10^8$   | $1.40 \times 10^8$ |
| $\text{M}_{4\text{-dcbpy}}$ <sup>[c]</sup> | 264.58                                    | $2.77 \times 10^9$   | $1.08 \times 10^9$ |
| $\text{M}_{4\text{-dmbpy}}$ <sup>[c]</sup> | 350.70                                    | $6.67 \times 10^8$   | $1.56 \times 10^8$ |
| $\text{M}_{5\text{-dmbpy}}$ <sup>[c]</sup> | 349.30                                    | $1.81 \times 10^8$   | $1.67 \times 10^8$ |

[a] 250  $\mu\text{M}$   $[\text{Ru}(\text{bpy})_3]^{2+}$  alone. [b] 250  $\mu\text{M}$   $\text{Co}_4\text{POM}$ . [c] 1 mM **M**. [d–e] See the Experimental Section for details on the calculation of PL lifetime and quenching rate coefficient. Note that  $[\text{Ru}(\text{bpy})_3]^{2+}$  has two different pathways for the quenching of its PL: oxidative quenching by electron acceptor like **M** and reductive quenching by electron donor like  $\text{Co}_4\text{POM}$ .<sup>[11b]</sup> The last two columns are the values of quenching rate coefficients ( $k_q$ ) calculated in terms of different unitless variables (i.e.,  $I_0/I$  and  $\tau_0/\tau$ ).

and the quenching rate constant of  $[\text{Ru}(\text{bpy})_3]^{2+}$  in the presence and absence of quenchers (as summarized in Table 1) and indirectly compare the efficiency of charge separation from excited  $[\text{Ru}(\text{bpy})_3]^{2+}$  to each quencher (i.e.,  $\text{Co}_4\text{POM}$  and  $\text{M}_{\text{bpy}}$ ). According to our results, the quenching rate constant of  $\text{Co}_4\text{POM}$  ( $1.33\text{--}6.97 \times 10^9 \text{ M}^{-1} \text{ s}^{-1}$ ) is much higher than that of  $\text{M}_{\text{bpy}}$  ( $1.40\text{--}3.23 \times 10^8 \text{ M}^{-1} \text{ s}^{-1}$ ) by approximately an order of magnitude, thus implying that the rate-limiting step is the electron transfer from photoexcited  $[\text{Ru}(\text{bpy})_3]^{2+}$  to  $\text{M}_{\text{bpy}}$  (i.e., reduction half reaction). The rate constant for  $\text{Co}_4\text{POM}$  calculated in the present study was found to be comparable to that reported previously for a similar tetranuclear polyoxometalate

$[\text{Ru}_4(\mu\text{-O})_4(\mu\text{-OH})_2(\text{H}_2\text{O})_4(\gamma\text{-SiW}_{10}\text{O}_{36})_2]^{10-}$  ( $\text{Ru}_4\text{POM}$ ;  $2.1\text{--}3.6 \times 10^9 \text{ M}^{-1} \text{ s}^{-1}$ ).<sup>[5d,e]</sup> According to Scandola and co-workers,<sup>[5d,e]</sup>  $\text{Ru}_4\text{POM}$  can act as an excellent hole scavenger for photogenerated oxidant. Owing to the difficulties in kinetically coupling photocatalytic oxidation with reduction half reactions, many researchers previously studied a half reaction by using a high concentration of sacrificial electron donor (e.g., triethylamine, triethanolamine, and ascorbic acid) or acceptors (e.g.,  $\text{H}_2\text{O}_2$ ,  $\text{S}_2\text{O}_8^{2-}$ ).<sup>[5b–e, 10b,c]</sup>

We found that the kinetic coupling of photocatalytic redox cycles for the complete artificial photosynthesis without sacrificial agents can be achieved by enhancing the charge-transfer efficiency of the rate-limiting step (i.e., between photoexcited dye and **M**) through chemical modification of **M** (Figure 2b–c). It was

hypothesized that **M** compounds with negatively chargeable functional groups, such as  $\text{COOH}$ , can facilitate the interaction between positively charged  $[\text{Ru}(\text{bpy})_3]^{2+}$  and **M**. As a proof of concept, we synthesized four kinds of cofactor regeneration catalysts that have a different functional group (R) on their bipyridine ligand ( $\text{M}_{\text{bpy}}$ ,  $\text{M}_{4\text{-dmbpy}}$ ,  $\text{M}_{5\text{-dmbpy}}$  and  $\text{M}_{4\text{-dcbpy}}$ ; Figure 2b) and investigated their effect on the quenching rate constant. Note that **M** compounds with other common functional groups, such as  $\text{NO}_2$ ,  $\text{NH}_2$ ,  $\text{SO}_3\text{H}$ , and  $\text{OH}$ , were excluded in this study because they exhibit poor catalytic activity and/or selectivity.<sup>[12b]</sup> According to our results (Figure 3a–b and Table 1), the nature of the functional groups on the bipyridine ligand of **M** significantly influences the quenching rate constant and the charge transfer efficiency between photoexcited  $[\text{Ru}(\text{bpy})_3]^{2+}$  and **M**.  $\text{M}_{4\text{-dcbpy}}$  had a high quenching rate constant ( $1.08\text{--}2.77 \times 10^9 \text{ M}^{-1} \text{ s}^{-1}$ ), comparable to that of  $\text{Co}_4\text{POM}$ , while other catalysts had much lower rate constants. These results support our hypothesis that electrostatic interaction between the dye and **M** can be used to improve the charge-transfer efficiency between them. Note that the  $\text{p}K_a$  value of  $\text{COOH}$  groups in the 4-dcbpy ligand was estimated to be 3.3–3.9 by Chemicalize (ChemAxon, Budapest, Hungary); thus, the 4-dcbpy ligand should be negatively charged at pH 7.4, as used in the present study. Our hypothesis is also supported by recent studies on the quenching behaviors of  $[\text{Ru}(\text{bpy})_3]^{2+}$ . According to literature,<sup>[5d,e, 13]</sup> positively charged  $[\text{Ru}(\text{bpy})_3]^{2+}$  can strongly interact with negatively charged species (e.g.,  $\text{S}_2\text{O}_8^{2-}$  and  $\text{Ru}_4\text{POM}$ ) even at a high ionic strength through electrostatic interactions, resulting in a high degree of PL quenching and a high quenching rate constant.

To demonstrate the kinetic coupling between the photocatalytic oxidation of water by  $\text{Co}_4\text{POM}$  and the reduction of nicotinamide cofactors by  $\mathbf{M}$ , we carried out experiments concerning photocatalytic regeneration of cofactors by using  $\mathbf{M}$  compounds containing different functional groups in the absence and presence of  $\text{Co}_4\text{POM}$  under the same conditions, so as to compare their regeneration efficiencies. As shown in Figure 3c–d, it was found that the efficiency of the photoregeneration of nicotinamide cofactor highly depended on the type of the functional group on the bipyridine ligand of  $\mathbf{M}$  as well as the presence of  $\text{Co}_4\text{POM}$  catalyst. Nicotinamide cofactor was efficiently photoregenerated only when  $\mathbf{M}_{4\text{-dcbpy}}$  and  $\text{Co}_4\text{POM}$  were used together, demonstrating the kinetic coupling between photocatalytic redox reactions. The order of the efficiency of NADH photoregeneration ( $\Phi_{\text{M}}$ ) was  $\mathbf{M}_{4\text{-dcbpy}} \gg \mathbf{M}_{4\text{-dmbpy}} > \mathbf{M}_{\text{bpy}} > \mathbf{M}_{5\text{-dmbpy}}$  whereas the order of catalytic activity ( $a_{\text{M}}$ ) was  $\mathbf{M}_{\text{bpy}} > \mathbf{M}_{4\text{-dcbpy}} > \mathbf{M}_{5\text{-dmbpy}} > \mathbf{M}_{4\text{-dmbpy}}$  (see the Supporting Information, Figure S8). Note that the catalytic activity of each  $\mathbf{M}$  was defined as the efficiency of NADH regeneration by electrochemical methods<sup>[14]</sup> (see experimental details in the Supporting Information). The observed mismatch between the orders of  $a_{\text{M}}$  and  $\Phi_{\text{M}}$  is attributed to different efficiencies of charge separation depending on the type of functional group on  $\mathbf{M}$ . We found that  $\Phi_{\text{M}}$  is almost linearly proportional to the product of  $a_{\text{M}}$  and the charge separation efficiency,  $\eta_{\text{CS}}$ , which is assumed to be proportional to the degree of PL quenching ( $q_{\text{M}}$ ) (see the Supporting Information, Figure S8). Note that  $\Phi_{\text{M}}$  can be expressed as in the following equation:  $\Phi_{\text{M}} = k\eta_{\text{LH}}\eta_{\text{CS}}a_{\text{M}}a_{\text{Co}_4\text{POM}}$ , where  $k$  is a proportional constant,  $\eta_{\text{LH}}$  is the light-harvesting efficiency of  $[\text{Ru}(\text{bpy})_3]^{2+}$ , and  $a_{\text{Co}_4\text{POM}}$  is the catalytic activity of  $\text{Co}_4\text{POM}$  against water splitting.

Based on these results, we attempted a coupling of nicotinamide cofactor photoregeneration with redox enzymatic synthesis of L-glutamate, a model chiral compound, by using L-glutamate dehydrogenase (GDH), a model redox enzyme (Figure 4a) that critically requires NADH for the reduction reaction. For comparison, we carried out photoenzymatic reactions with two types of electron donors: water with a  $\text{Co}_4\text{POM}$  water-splitting catalyst and a common electron donor triethanolamine (TEOA) without the catalyst. According to our results (Figure 4b),  $\mathbf{M}_{4\text{-dcbpy}}$  has the highest efficiency for the photoregeneration of NADH regardless of the type of electron donor. The regeneration efficiency (10.7%) obtained with  $\text{Co}_4\text{POM}$  was much lower than that by using TEOA (70.7%); however, considering the low concentration of  $\text{Co}_4\text{POM}$  (250  $\mu\text{M}$ ) and the presence of molecular oxygen when using water as an electron donor, it was thought that the overall efficiency of the system using  $\text{Co}_4\text{POM}$  is higher than or at least comparable to that using TEOA even though the oxidation of water (four-electron process) is much more difficult than that of TEOA (one-electron process). It was previously reported that the catalytic activity of  $\mathbf{M}$  can be significantly degraded by molecular oxygen.<sup>[12]</sup> Based on these results, we further tested only  $\mathbf{M}_{4\text{-dcbpy}}$  for the photoenzymatic synthesis of L-glutamate. As shown in Figure 4c, we could successfully photosynthesize L-glutamate through reductive amination of  $\alpha$ -ketoglutarate under visible light by using water as an electron donor. Considering that  $\mathbf{M}$

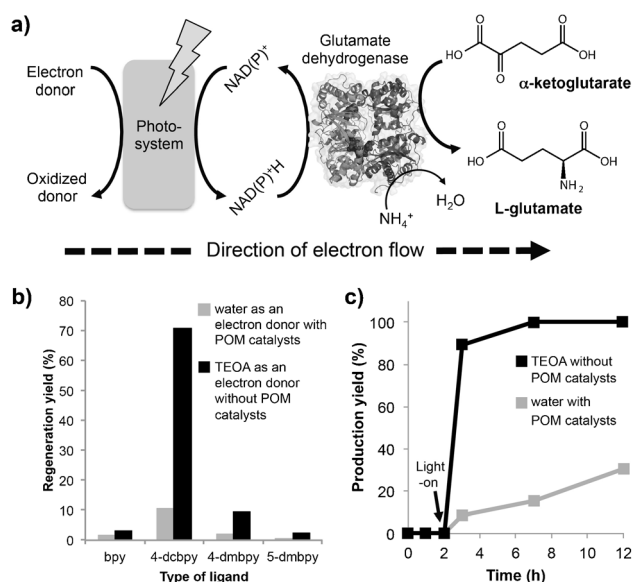


**Figure 4.** Photoenzymatic synthesis of L-glutamate using glutamate dehydrogenase. a) Scheme showing catalytic cycles of the photoenzymatic reaction. b) Photoregeneration of NADH using different electron donors (i.e., water and TEOA). c) Photoenzymatic synthesis of L-glutamate through in situ regeneration of NADH by complete artificial photosynthesis: simultaneous photocatalytic oxidation of water and reduction of NADH cofactors. Note that before the regeneration test, reaction media were degassed.

compounds can also regenerate other enzyme cofactors, such as NADPH and FADH,<sup>[12]</sup> in principle, our system can be applied to any kind of cofactor-dependent redox biocatalysis for the synthesis of complex chiral compounds and valuable drug intermediates reported in the literature.<sup>[15]</sup> In addition to industrial potential, we believe that the present study is a scientific milestone as the first example of artificial photosynthesis achieved by the integral coupling of water splitting with a biocatalytic reaction.

In summary, we have developed a new type of artificial photosynthesis system that couple photocatalytic and biocatalytic cycles by using water as an electron donor under ambient conditions. The system was designed to regenerate (i.e., reduce) cofactors by photocatalytic cycles and to consume (i.e., oxidize) the regenerated cofactors by biocatalytic cycles for enzymatic synthesis of target chemicals. The photocatalytic system for cofactor regeneration consisted of light-harvesting dye  $[\text{Ru}(\text{bpy})_3]^{2+}$ , water splitting catalyst  $\text{Co}_4\text{POM}$  as a hole scavenger, and a cofactor regeneration catalyst  $\mathbf{M}$  as an electron scavenger. According to our dynamic and static photoluminescence studies, charge-transfer efficiency from the photoexcited dyes to conventional  $\mathbf{M}$  is much lower than that to  $\text{Co}_4\text{POM}$ .  $\mathbf{M}$  compounds with a negatively chargeable COOH group led to a significant enhancement of the efficiency of the charge transfer from the dyes to  $\mathbf{M}$  through electrostatic interaction, allowing kinetic coupling of photocatalytic redox cycles. We could successfully regenerate nicotinamide cofactors through simultaneous photocatalytic oxidation of water and the reduction of cofactors, which were then used for redox enzymatic synthesis of L-glutamate. Considering the high potential of redox biocatalysis for the synthesis of complex chemicals, this study can

provide a new horizon for the realization of artificial photosynthesis technology.

## Experimental Section

### Materials

All chemicals, including  $\text{RhCl}_3 \cdot 3\text{H}_2\text{O}$ , hexamethyldearbenzene (HMDB), 2,2'-bipyridine (bpy), 4,4'-dimethyl-2,2'-bipyridine (4-dmbpy), 5,5'-dimethyl-2,2'-bipyridine (5-dmbpy), 4,4'-dicarboxy-2,2'-bipyridine (4-dcbpy), methanol, *N,N*-dimethylformamide, diethyl ether, chloroform, benzene,  $\text{NAD}^+$ , triethanolamine (TEOA),  $\alpha$ -ketoglutarate, glutamate dehydrogenase (GDH),  $\text{Na}_2\text{WO}_4 \cdot 3\text{H}_2\text{O}$ ,  $\text{Na}_2\text{HPO}_4 \cdot 7\text{H}_2\text{O}$ ,  $\text{Co}(\text{NO}_3)_2 \cdot 6\text{H}_2\text{O}$ , and tris(2-2'-bipyridyl)dichlororuthenium(II) hexahydrate ( $\text{Ru}(\text{bpy})_3\text{Cl}_2 \cdot 6\text{H}_2\text{O}$ ) were purchased from Sigma-Aldrich (St. Louis, MO).

### Synthesis of $[\text{Cp}^*\text{Rh}(\text{bpy})(\text{H}_2\text{O})]^{2+}$ and derivatives thereof

Details of the method for the synthesis of  $[\text{Cp}^*\text{Rh}(\text{bpy})(\text{H}_2\text{O})]^{2+}$  and its derivatives can be found elsewhere.<sup>[12]</sup> Briefly,  $\text{RhCl}_3 \cdot 3\text{H}_2\text{O}$  (1 mmol) and hexamethyldearbenzene (HMDB) (2.5 mmol) were dissolved in anhydrous methanol and then refluxed at 65 °C for 15 h under vigorous stirring in Ar atmosphere. A brown solid product was recovered by rotary evaporation and then redissolved in chloroform. Byproducts were removed by washing with an excess amount of deionized water. The intermediate product  $[\text{Cp}^*\text{RhCl}_2]$  ( $\text{Cp}^*$  = pentamethylcyclopentadienyl) was further purified by crystallization in chloroform/benzene (1:10).  $[\text{Cp}^*\text{Rh}(\text{bpy})(\text{H}_2\text{O})]^{2+}$  and its derivatives (**M**) were prepared by mixing  $[\text{Cp}^*\text{RhCl}_2]$  and two equimolar amounts of bipyridine derivatives (e.g., bpy, 4-dmbpy, 5-dmbpy, or 4-dcbpy) in methanol or *N,N*-dimethylformamide for 1 h. Final products were separated by crystallization in methanol/diethyl ether (1:5), dried under vacuum overnight, and characterized by FT-IR spectroscopy (see the Supporting Information, Figure S1) and cyclic voltammetry (see the Supporting Information, Figure S2).

### Synthesis of water-splitting catalyst $[\text{Co}_4(\text{H}_2\text{O})_2(\text{PW}_9\text{O}_{34})_2]^{10-}$ (**Co<sub>4</sub>POM**)

Tetracobalt polyoxometalates,  $[\text{Co}_4(\text{H}_2\text{O})_2(\text{PW}_9\text{O}_{34})_2]^{10-}$ , was prepared according to the literature.<sup>[5b]</sup> In brief, the sodium salt of **Co<sub>4</sub>POM** ( $\text{Na}_{10}\text{-Co}_4\text{POM}$ ) was synthesized by refluxing an aqueous solution (100 mL, pH 7) of  $\text{Na}_2\text{WO}_4 \cdot 3\text{H}_2\text{O}$  (0.108 mol),  $\text{Na}_2\text{WO}_4 \cdot 3\text{H}_2\text{O}$  (0.012 mol),  $\text{Na}_2\text{HPO}_4 \cdot 7\text{H}_2\text{O}$ , and  $\text{Co}(\text{NO}_3)_2 \cdot 6\text{H}_2\text{O}$  (0.024 mol) at 100 °C for 2 h. The resulting **Co<sub>4</sub>POM** was separated by precipitation by addition of excessive amounts of NaCl, further purified by recrystallization from hot water, and characterized by various analytical tools, such as FT-IR/Raman spectroscopy, UV/Vis absorption spectroscopy, and cyclic voltammetry (see the Supporting Information, Figures S3–S6).

### Spectroscopic analysis

Cofactor regeneration catalyst **M** (see the Supporting Information, Figure S1) and water-splitting catalyst **Co<sub>4</sub>POM** (see the Supporting Information, Figure S3) were analyzed by using a Hyperion 3000 FT-IR spectrometer (Bruker Optics, Ettlingen, Germany) by the KBr pellet method under vacuum and a LabRAM HR UV/Vis/NIR dispersive Raman microscope (Horiba Jobin Yvon, Kyoto, Japan) under the following conditions: number of scan, 128; scan range, 400–4,000  $\text{cm}^{-1}$ ; resolution, 4  $\text{cm}^{-1}$ ; Ar ion laser (514.5 nm) for Raman spectroscopy. Absorbance spectra of **Co<sub>4</sub>POM** (see the Supporting

Information, Figure S4) and  $[\text{Ru}(\text{bpy})_3]^{2+}$  were measured by using a Jasco V-650 spectrophotometer (Tokyo, Japan).

### Cyclic voltammetry

Electrochemical activities of **Co<sub>4</sub>POM** (see the Supporting Information, Figure S5) and **M** compounds (see the Supporting Information, Figure S2) were examined by cyclic voltammetry by using a 273 A potentiostat/galvanostat (Princeton Applied Research, Oak Ridge, TN) in a 3-electrode configuration: GC disk (0.03  $\text{cm}^2$ ) as a working electrode, Pt wire as a counter electrode, and Ag/AgCl as a reference electrode.

### Photocatalytic splitting of water by using **Co<sub>4</sub>POM**

Photocatalytic oxygen evolution from water by **Co<sub>4</sub>POM** was tested under the following conditions: 1 mM  $[\text{Ru}(\text{bpy})_3]^{2+}$  as a light-harvesting dye, 10  $\mu\text{M}$  **Co<sub>4</sub>POM** as a water-splitting catalyst, and 5 mM  $\text{Na}_2\text{S}_2\text{O}_8$  as an electron scavenger in 80 mM sodium borate buffer (pH 8.0). Before visible-light irradiation, the above solution was purged with Ar gas for 30 min in a gas-tight vial. For the analysis of  $\text{O}_2$  evolution, 250  $\mu\text{L}$  of samples were taken from the headspace of the vial every 10 min after light irradiation by using an air-tight syringe and measured with an Agilent 7890 A gas chromatograph equipped with a thermal conductivity detector (see the Supporting Information, Figure S6).

### Photoluminescence characterization of $[\text{Ru}(\text{bpy})_3]^{2+}$

Photoluminescence (PL) quenching of  $[\text{Ru}(\text{bpy})_3]^{2+}$  (250  $\mu\text{M}$  in 0.1 M phosphate buffer, pH 7.4) was studied by measuring its static and dynamic (time-resolved) PL spectra in the presence and absence of quenchers: **M** (1 mM; Figure 3) and **Co<sub>4</sub>POM** (250  $\mu\text{M}$ ; see the Supporting Information, Figure S7). Static PL spectra were measured with a Shimadzu RF5301-PC spectrofluorometer (Tokyo, Japan). Dynamic PL spectra were measured at 600 nm under excitation at 450 nm with a pulsed laser diode (pulsed width < 1.3 ns) by using a Horiba NanoLog spectrofluorometer (Kyoto, Japan). The PL lifetime ( $\tau$ ) of  $[\text{Ru}(\text{bpy})_3]^{2+}$  was determined by fitting time-resolved PL decay curves by using the following equation:  $I = A\text{exp}(-t/\tau)$  where  $t$  is a given time,  $A$  is an exponential prefactor that was normalized to unity, and  $\tau$  is the lifetime (Table 1). Quenching rate coefficients were calculated by the Stern–Volmer relationship:  $I_0/I = \tau_0/\tau = 1 + k_q\tau_0[Q]$  where  $I_0$  and  $I$  are the PL intensity of  $[\text{Ru}(\text{bpy})_3]^{2+}$  without and with a quencher, respectively,  $\tau_0$  and  $\tau$  are the PL lifetime of  $[\text{Ru}(\text{bpy})_3]^{2+}$  without and with a quencher, respectively,  $k_q$  is the quenching rate coefficient, and  $[Q]$  is the concentration of the quencher.

### Photochemical reactions

Photoregeneration of NADH was carried out in the presence and absence of the water-splitting catalyst **Co<sub>4</sub>POM**. The reaction medium (pH 7.4) consisted of  $\text{NAD}^+$  (1 mM), **M** (1 mM),  $[\text{Ru}(\text{bpy})_3]^{2+}$  (250  $\mu\text{M}$ ), and phosphate buffer (100 mM). **Co<sub>4</sub>POM** (250  $\mu\text{M}$ ) can be additionally dissolved in the reaction medium for the photoregeneration of NADH coupled with water splitting. For comparison, triethanolamine (TEOA, 1 M) was used as a sacrificial electron donor in the absence of **Co<sub>4</sub>POM**. The regeneration of NADH from  $\text{NAD}^+$  was monitored by measuring the change of optical density of the reaction medium at 340 nm. Note that the molar absorption coefficient of NADH at 340 nm is  $6.22 \times 10^3 \text{ M}^{-1} \text{ cm}^{-1}$ . For the synthesis of model chiral compound L-glutamate, NADH-dependent glutamate dehydrogenase (GDH) was

used as a model redox enzyme under the following conditions:  $\text{NAD}^+$  (1 mM), **M** (1 mM),  $[\text{Ru}(\text{bpy})_3]^{2+}$  (250  $\mu\text{M}$ ),  $\text{Co}_4\text{POM}$  (250  $\mu\text{M}$ ),  $\alpha$ -ketoglutarate (5 mM),  $(\text{NH}_4)_2\text{SO}_4$  (100 mM), GDH (40 U), and phosphate buffer (0.1 M, pH 7.4). Photoenzymatic synthesis of L-glutamate from  $\alpha$ -ketoglutarate was analyzed with a Shimadzu LC-20 A high-performance liquid chromatograph (Tokyo, Japan). Throughout the whole photochemical reaction, reaction media were irradiated with a xenon lamp (450 W) through a 420 nm cut-off filter.

### Electrochemical regeneration of NADH

A constant potential of  $-0.8$  V versus Ag/AgCl was applied to electrochemically regenerate NADH cofactors.<sup>[14]</sup> The reaction medium for the electrochemical regeneration of NADH cofactors was composed of 1 mM  $\text{NAD}^+$  and 1 mM **M** in 0.1 M phosphate buffer (pH 7.4). The electrochemical regeneration of NADH was carried out under deaerated conditions.

### Acknowledgements

This study was supported by grants from the National Research Foundation (NRF) through the National Leading Research Laboratory (NRF-2013R1A2A1A05005468) and the Intelligent Synthetic Biology Center of Global Frontier R&D Project (2011-0031957), Republic of Korea

**Keywords:** biocatalysis · NADH · photosynthesis · redox enzymes · water splitting

- [1] a) R. E. Blankenship, *Molecular Mechanisms of Photosynthesis*, Blackwell Science, Oxford, **2002**; b) A. F. Collings, C. Critchley, *Artificial Photosynthesis: From Basic Biology to Industrial Application*, Wiley-VCH, Weinheim, **2005**.
- [2] a) G. D. Scholes, G. R. Fleming, A. Olaya-Castro, R. van Grondelle, *Nat. Chem.* **2011**, *3*, 763–774; b) K. N. Ferreira, T. M. Iverson, K. Maghlaoui, J. Barber, S. Iwata, *Science* **2004**, *303*, 1831–1838.
- [3] a) A. J. Bard, M. A. Fox, *Acc. Chem. Res.* **1995**, *28*, 141–145; b) N. S. Lewis, D. G. Nocera, *Proc. Natl. Acad. Sci. USA* **2006**, *103*, 15729–15735; c) L. Vayssieres, *On Solar Hydrogen & Nanotechnology*, John Wiley & Sons, Singapore, **2009**.
- [4] a) F. Gloaguen, T. B. Rauchfuss, *Chem. Soc. Rev.* **2009**, *38*, 100–108; b) F. Wang, W.-G. Wang, X.-J. Wang, H.-Y. Wang, C.-H. Tung, L.-Z. Wu, *Angew. Chem. Int. Ed.* **2011**, *50*, 3193–3197; c) M. L. Helm, M. P. Stewart, R. M. Bullock, M. R. Dubois, D. L. Dubois, *Science* **2011**, *333*, 863–866.

- [5] a) M. W. Kanan, D. G. Nocera, *Science* **2008**, *321*, 1072–1075; b) Q. Yin, J. F. Tan, C. Besson, Y. V. Geletii, D. G. Musaev, A. E. Kuznetsov, Z. Lou, K. I. Hardcastle, C. L. Hill, *Science* **2010**, *328*, 342–345; c) Z. Huang, Z. Luo, Y. V. Geletii, J. W. Vickers, Q. Yin, D. Wu, Y. Hou, Y. Ding, J. Song, D. G. Musaev, C. L. Hill, T. Lian, *J. Am. Chem. Soc.* **2011**, *133*, 2068–2071; d) M. Orlandi, R. Argazzi, A. Sartorel, M. Carraro, G. Scorrano, M. Bonchio, F. Scandola, *Chem. Commun.* **2010**, *46*, 3152–3154; e) M. Natali, M. Orlandi, S. Berardi, S. Campagna, M. Bonchio, A. Sartorel, F. Scandola, *Inorg. Chem.* **2012**, *51*, 7324–7331.
- [6] a) C. Tard, C. J. Pickett, *Chem. Rev.* **2009**, *109*, 2245–2274; b) D. W. Mulder, E. S. Boyd, R. Sarma, R. K. Lange, J. A. Endrizzi, J. B. Broderick, J. W. Peters, *Nature* **2010**, *465*, 248–252.
- [7] J. P. McEvoy, G. W. Brudvig, *Chem. Rev.* **2006**, *106*, 4455–4483.
- [8] a) C. M. Drain, A. Varott, I. Radivojevic, *Chem. Rev.* **2009**, *109*, 1630–1658; b) Y. S. Nam, T. Shin, H. Park, A. P. Magyar, K. Choi, G. Fantner, K. A. Nelson, A. M. Belcher, *J. Am. Chem. Soc.* **2010**, *132*, 1462–1463.
- [9] P. Yang, J.-M. Tarascon, *Nat. Mater.* **2012**, *11*, 560–563.
- [10] a) S. H. Lee, J. H. Kim, C. B. Park, *Chem. Eur. J.* **2013**, *19*, 4392–4406; b) S. H. Lee, D. H. Nam, J. H. Kim, J.-O. Baeg, C. B. Park, *ChemBioChem* **2009**, *10*, 1621–1624; c) L. L. Tinker, N. D. McDaniel, S. Bernhard, *J. Mater. Chem.* **2009**, *19*, 3328–3337; d) S. H. Lee, D. H. Nam, C. B. Park, *Adv. Synth. Catal.* **2009**, *351*, 2589–2594; e) J. Ryu, S. H. Lee, D. H. Nam, C. B. Park, *Adv. Mater.* **2011**, *23*, 1883–1888; f) S. H. Lee, J. Ryu, D. H. Nam, C. B. Park, *Chem. Commun.* **2011**, *47*, 4643–4645; g) J. H. Kim, M. Lee, J. S. Lee, C. B. Park, *Angew. Chem. Int. Ed.* **2012**, *51*, 517–520; *Angew. Chem.* **2012**, *124*, 532–535; h) D. H. Nam, C. B. Park, *Chembiochem* **2012**, *13*, 1278–1282; i) J. H. Kim, D. H. Nam, C. B. Park, *Curr. Opin. Biotechnol.* **2014**, *28*, 1–9.
- [11] a) N. H. Damrauer, G. Cerullo, A. Yeh, T. R. Bousie, C. V. Shank, J. K. McCusker, *Science* **1997**, *275*, 54–57; b) S. Campagna, F. Puntoriero, F. Nastasi, G. Bergamini, V. Balzani, *Top. Curr. Chem.* **2007**, *280*, 117–214.
- [12] a) H. C. Lo, O. Buriez, J. B. Kerr, R. H. Fish, *Angew. Chem.* **1999**, *111*, 1524–1527; *Angew. Chem. Int. Ed.* **1999**, *38*, 1429–1432; b) F. Hildebrand, C. Kohlmann, A. Franz, S. Lutz, *Adv. Synth. Catal.* **2008**, *350*, 909–918.
- [13] E. M. Tuite, D. B. Rose, P. M. Ennis, J. M. Kelly, *Phys. Chem. Chem. Phys.* **2012**, *14*, 3681–3692.
- [14] a) H.-K. Song, S. H. Lee, K. Won, J. H. Park, J. K. Kim, H. Lee, S.-J. Moon, D. K. Kim, C. B. Park, *Angew. Chem.* **2008**, *120*, 1773–1776; *Angew. Chem. Int. Ed.* **2008**, *47*, 1749–1752; b) S. H. Lee, K. Won, H.-K. Song, C. B. Park, *Small* **2009**, *5*, 2162–2166.
- [15] a) G. A. Strohmeier, H. Pichler, O. May, M. Gruber-Khadjawi, *Chem. Rev.* **2011**, *111*, 4141–4164; b) M. Hall, A. S. Bommarius, *Chem. Rev.* **2011**, *111*, 4088–4110; c) F. Hollmann, I. W. C. E. Arends, K. Buehler, *ChemCatChem* **2010**, *2*, 762–782.

Received: April 29, 2014

Published online on August 1, 2014